Materials and Design 201 (2021) 109509

Contents lists available at ScienceDirect

Materials and Design

journal homepage: www.elsevier.com/locate/matdes

Moiré pattern at graphene/Al (111) interface: Experiment and simulation

Shuang Zhang [a,1], Dongjun He [a,1], Ping Huang [a,*], Fei Wang [b]

[a] State Key Laboratory for Mechanical Behavior of Materials, School of Materials Science and Engineering, Xi'an Jiaotong University, Xi'an City 710049, PR China
[b] State Key Laboratory for Strength and Vibration of Mechanical Structures, School of Aerospace Engineering, Xi'an Jiaotong University, Xi'an City 710049, PR China

HIGHLIGHTS

- Moiré pattern at Al/graphene interface was achieved in the first time.
- The periodicity of the moiré pattern is unexpected large in Al/graphene interface.
- Thermal stress stimulated interface rotation dominates the unusual moiré pattern.
- Path a new way to design and alter moiré pattern in metal/graphene materials system.

GRAPHICAL ABSTRACT

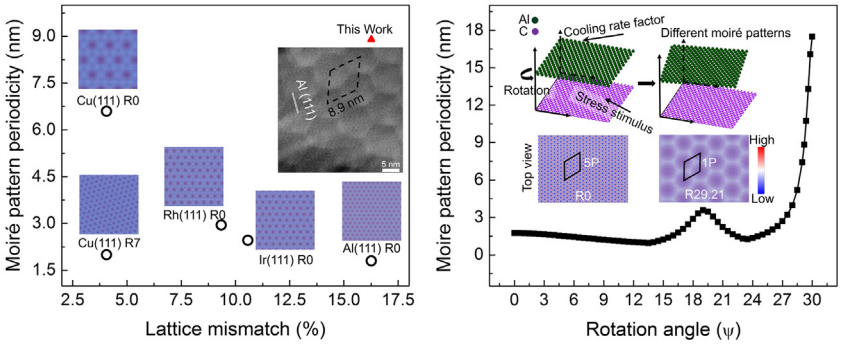

ARTICLE INFO

Article history:
Received 26 November 2020
Received in revised form 10 January 2021
Accepted 19 January 2021
Available online 22 January 2021

Keywords:
Graphene/Al (111) interface
Large moiré pattern periodicity
Interface interaction
Molecular dynamics simulation

ABSTRACT

Moiré pattern periodicity associated with interface interaction that reflects intrinsic interface characteristics strongly affects the electronic/chemical/mechanical properties in numerous metal/graphene systems. Despite intensive researches were conducted on graphene/Al composites, however, no moiré patterns have ever been reported in their graphene/Al interfaces. In the present study, through vacuum arc melting and suction casting technique, moiré pattern with unexpected large periodicity of ~8.9 nm has been observed at graphene/Al (111) interface for the first time. The moiré pattern periodicity with respect to rotation orientation angle was evaluated by theoretical calculation; and the formation process of the moiré pattern was investigated via molecular dynamics simulations. Thermal stress stimulated interface rotational growth was proposed to play a dominating role and a tentative interface interaction analysis concerned on the unusual moiré pattern at the graphene/Al (111) interface was illustrated. The experiments along with theoretical and simulation study focused on the moiré pattern formed at graphene/Al interface may path a way to tailor interface structures of graphene/metal materials systems

1. Introduction

Graphene is well known as a two-dimensional (2D) material with fantastic physicochemical properties such as high carrier mobility, thermal transport, and ultra-high mechanical strength [1,2], that makes graphene attractive for applications in nanoelectromechanical devices [3], in high-performance low-power electronics [4], and as transparent electrodes [5]. Interfacing graphene with metals (e.g., substrates, electrodes and matrix) is a prerequisite for various practical applications. Consequently, graphene/metal interface forms and thus translating intriguing properties of graphene from nanoscale to the macroscopic world as well as triggering unexpected functionalities to the graphene/metal systems [6–9]. Therefore, graphene/metal systems overall performance is substantially dependent on the nature of graphene/metal

* Corresponding author.
E-mail address: huangping@mail.xjtu.edu.cn (P. Huang).
[1] These authors contributed equally to this work

https://doi.org/10.1016/j.matdes.2021.109509

interface, e.g., the mechanical, rich electronic and chemical properties induced at the interfaces [2,10–14]. An important characteristic of the graphene/metal interface is the formation of moiré pattern, i.e. the expression of a superperiodicity upon superimposing two similar spatial distribution periodic structures.

Recently, moiré pattern has become excellent platforms for investigating new properties of two-dimensional (2D) layered materials. It has reported periodic moiré patterns can induce structural altering and band transformations, generating new phenomena including moiré phonons [15], moiré excitons [16], and unconventional superconductivity [17]. Prevalently, moiré pattern also has been widely reported on many metals [2,12,18], such as Cu [19,20], Ni [21], Ag [22], Au [23], Pd [24], Pt [25,26], Rh [27,28], Ir [29], Co [30] and Ru [31], and those studies have revealed moiré pattern associated with interface interaction could reflect intrinsic interface characteristics with relation to optical, chemical, electronic and magnetic properties [11,12]. Varying moiré pattern periodicity strongly affects these properties of metal/graphene systems, as well as the moiré pattern periodicity can be tuned by lattice mismatch [23] and rotation orientation angle [29,32,33]. Above all, the knowledge of graphene/metal interface with moiré pattern characteristic is significant to both fundamental studies and applications of graphene/metal materials. Even though tremendous efforts were conducted on elemental Al and Al alloys in both scientific and industrial field, intriguingly, no moiré pattern ever reported in graphene/Al interface yet.

Generally, the moiré pattern has been observed at the interface grown by epitaxy graphene on metals in a "bottom-up" manner by scanning tunneling microscopy (STM) measurements, which benefits from the high-temperature tolerance of metallic substrates, active carbon-catalyst metal surfaces (e.g., Ni, Co, Ru etc.) or low carbon solubility (e.g., Cu, Au, Pt etc.). Whereas the epitaxial growth of graphene on Al is absent might because of poor catalytic activity of Al in dissociating hydrocarbons, together with the low melting temperature of Al, thus unfavorable to act as a substrate, hence lack of awareness of moiré pattern interface for graphene on Al substrate. Moreover, regard to tremendous efforts conducted in graphene reinforced Al composites [9,12,34–38], the graphene/Al interface is introduced by "top-down" approaches, consequently the investigation and understanding of the graphene/Al interface are rather limited because examining the interfacial structure and properties in bulk materials is complex, e.g., the formation of metal carbides/oxides [35,39], or delamination due to the poor wetting of Al with graphene [40]. Hence, due to the limitation of objective conditions, those issues increase the difficulty in understanding the moiré pattern at graphene/Al interface.

Since the moiré pattern related physicochemical characteristics is critical to the performance of graphene/Al systems. Each moiré unit cell can be divided into several regions of different arrangement of graphene atoms with respect to metal atoms [41]. The mutual arrangement determines the local distance and interaction strength between graphene and substrate [27,42–45], and a small interfacial adjustment in graphene reinforced metallic matrix composites (GRMMCs) can make big differences in electronic structure [46]. For better understanding the graphene/Al interface and related properties, the forming of specific moiré pattern periodicity interface, the mysterious moiré pattern characteristics, moiré pattern related interface interactions (the work of adhesion/interface energy) should be discussed for fundamental understanding.

In the present study, moiré pattern has been successfully observed in graphene/Al (111) composites fabricated through vacuum arc melting and suction casting technique via transmission electron microscopy (TEM) observation for the first time. Also, the moiré pattern periodicity derived here is unexpected to be ~8.9 nm that is larger than those observed in other metal/graphene systems. Then, the moiré pattern in graphene/Al composites is evaluated and confirmed by both theory calculations and molecular dynamics (MD) simulations, demonstrating the interfacial rotation induced by thermal stress upon rapid cooling is the underlying mechanism that responsible to the large periodic moiré pattern at graphene/Al interface. Finally, a tentative interface interaction analysis of the moiré pattern at the graphene/Al (111) interface is illustrated. Consequently, the results can shed light on the foundational interface-property relationship of graphene reinforced Al composites.

2. Experiments

2.1. Materials preparation and characterization

Graphene reinforced Al composites were fabricated through a vacuum arc melting and suction casting method via two steps: the pre-dispersion of the graphene nanosheets in the Al powders and the casting of the pre-dispersion graphene/Al composite powders. The pre-dispersion of graphene nanosheets among Al powders is based on electrostatic adsorption between graphene and Al under Alcohol solution [47]. Specifically, the graphene nanosheets (GNSs, 99.5% purity, obtained from Nanjing XFNano Material Tech Co. Ltd. China) were firstly dispersion in 90% alcohol solution under ultrasonic homogenizer for 30 min to form a uniform suspension. After that, Al powders (99.99% purity, 15.22 μm average particle size, Beijing Yanbang new material company Co. Ltd., China) were added slowly into the GNSs suspension. The mixed slurry was mixed under magnetic stirring (400 r/min) in ultrasonic bath for 30 min. Next, the pre-dispersion graphene/Al composite powders were immediately prepared by suction filtration of mixed slurry and dried at 323 K under vacuum for 12 h. Finally, the quality of graphene in composite powders was characterized by Raman spectrum (Fig. S1).

During casting of the pre-dispersion graphene/Al composite powders, the graphene/Al composite powders were packaged by Al foil for the sake of avoiding blow away. Then ensure that the vacuum of the arc melting furnace is lower than 5×10^{-3} Pa, afterwards pass in 0.5–0.6 Pa Ar gas. A direct current (DC) of 150 A and 8 V are applied through the tungsten cathode to the composite powders in a pulsed mode with 2 min on and 1 min off in a vacuum arc melting furnace, and the graphene/Al mixture is simultaneously stirred by magnetic stirring for several minutes to obtain uniform distribution of the GNSs in the metal. The whole melting process repeated three to five times depending on fabrication conditions. Then the molten mixture was solidified by suction casting in a copper mould for rapid solidification molding. Thus the graphene/Al bulk composites were successfully prepared.

Then, in order to characterize the microstructure of graphene/Al interface, the sample was characterized by TEM instrument (JEOL JEM-2100Plus). Specimens for TEM were prepared by twin-jet electropolisher method with a large thin area. The detailed steps are as follows: first a small piece cut out from the graphene/Al bulk samples obtained by suction casting which was then thinned to 60–80 μm by mechanical polishing, and then punch the sample into a 3 mm diameter disc. Finally, the sample was clamped into the central position of the electrolytic cell and thinned by twin-jet electropolisher under 5% perchloric acid alcohol solution at −40°C.

2.2. Molecular dynamics simulations

The graphene/Al composite growth process and graphene/Al interface characteristics were performed with molecular dynamics simulations via LAMMPS [48]. Two different models were created to describe the formation process and evaluate graphene/Al interface configuration (models and details are shown in Figs. S3-S7). Graphene/Al models adopted hybrid pair-style interaction. The embedded atom method (EAM) interatomic potentials with Finnis-Sinclair as given by Mendelev [49] and EAM interatomic potentials by Mishin [50] et al. were chosen to describe the interaction between Al atoms in the formation process and interface feature calculation process, respectively. Carbon atoms

were described by adaptive intermolecular reactive empirical bond-order potential (AIREBO) [51]. The Lennard-Jones (LJ) type of van der Waals interaction was used to describe the interactions between Al and graphene atoms and the parameters were $\varepsilon = 0.035078$ eV and $\sigma = 3.0135$ Å [52]. Periodic boundary conditions (PPP) were applied for *x*-, *y*- and *z*- directions in the above two simulation systems, i.e., graphene/Al interface formation model and interface configuration calculation model. The open visualization tool OVITO developed by Stukowski [53] is used to visualize the atomic structure.

3. Results and discussion

3.1. The moiré pattern at graphene/Al interface by experiments

The microstructural features of graphene/Al interface are shown in Fig. 1(a), in which the dark shaded area on the left is identified to be graphene surrounded by Al matrix, showing periodic moiré pattern formed at the interface. Fig. 1(b) shows the corresponding high resolution TEM of selected region of Fig. 1(a). Clearly, the crystal with an interplanar spacing of 0.23 nm corresponds to Al (111), and the average moiré pattern periodicity of all the hexagonal rings is estimated to be ~8.9 nm. The rather large periodicity is unusual, as the larger lattice mismatch ($\delta_{Al} = 16.16\%$) of graphene/Al interface should result in small moiré pattern periodicity of ~1.15 nm predicted by simulation [54]. To our best of knowledge, it is the first time to report the moiré pattern in graphene/Al systems by experiments. Though plenty of graphene/Al composites have been prepared through "top-down" strategy, moiré pattern interfaces have hardly been observed, even clear TEM images of the graphene/metal interface are rarely reported. The present clear moiré pattern interface image might depend on the high quality of graphene (Fig. S1) and rapid solidification achieved through vacuum arc melting and suction casting furnace with avoiding interfacial reaction. The lattice of graphene is difficult to observe as has been reported in many literatures [12,55]. Whatever, some enlarged images of other small areas of graphene/Al interface are presented in Fig. S2, showing other interface characteristic morphology with no moiré pattern interface characteristics.

3.2. Moiré pattern periodicity determined via theory calculation

As the moiré pattern periodicity has relation to not only lattice mismatch but also rotation orientation angle [29,32,56,57], the moiré pattern periodicities reported by literatures [2,20,29,58,59] are plotted, with present moiré pattern periodicity, as shown in Fig. 2, in which R0 refers to rotation angle of 0 degree and identical nomenclature is used for other angles. As demonstrated in the insets that the moiré pattern atomic models for each graphene/metal interfaces, moiré pattern periodicity is varying with either lattice mismatch or rotation angle, that is, larger lattice mismatch results in smaller moiré pattern periodicity besides a small rotation angle adjustment makes big change in moiré pattern periodicity. Moreover, by tuning the lattice mismatch [23] or rotation orientation [7,19] angle at the same graphene/metal interface could achieve changeable moiré pattern periodicity. For example, in graphene/Au system [23] the large moiré pattern periodicity was attributed to surface reconstruction mechanism with reduced lattice misfit between graphene and Au derived from lattice distortion/strain during moderate annealing treatment. However, it is not the case in the present study since the current fabrication condition underwent rapid melting/solidification process, which means the surface reconstruction mechanism can hardly be suitable for so large moiré pattern periodicity at graphene/Al interface, for the reason of requiring very large misfit variation from interface strain in bulk materials. Therefore, the large moiré pattern periodicity of ~8.9 nm observed in the present graphene/Al interface may attribute to the rotational growth between Al matrix and graphene layers, as proposed previously in graphene/Cu (111) and graphene/Ir (111) [29,57]. As indicated in the following, indeed, the interface of graphene/Al could achieve different moiré pattern periodicities at distinct rotation angles. Considering the *x*-axis [1−10] of the Al (111) plane aligned with the zigzag direction of graphene to be the rotation angle of 0, based on the theoretical calculation proposed in ref. [32], the moiré pattern periodicity of ~8.9 nm is estimated to correspond to be rotation angle of 29.21° (see Supplementary Information S5 for details).

Moreover, the moiré pattern periodicity derived via theory calculation as a function of rotation angle for graphene/Al interface is shown in Fig. 3, in which interface configurations correspond to various moiré pattern periodicities with rotation angles are displayed. Green atoms represent Al atoms, purple atoms represent graphene atoms and black curve means theoretical moiré pattern periodicities varying upon rotation angles. The moiré pattern periodicity maintains a small value (< 4 nm) for the rotation range from 0° to 28°, while the periodicity sharply rises from 28° to 30°, and reaches the largest moiré pattern periodicity at 30° rotation angle. Also, the insets of (a)-(e) demonstrate

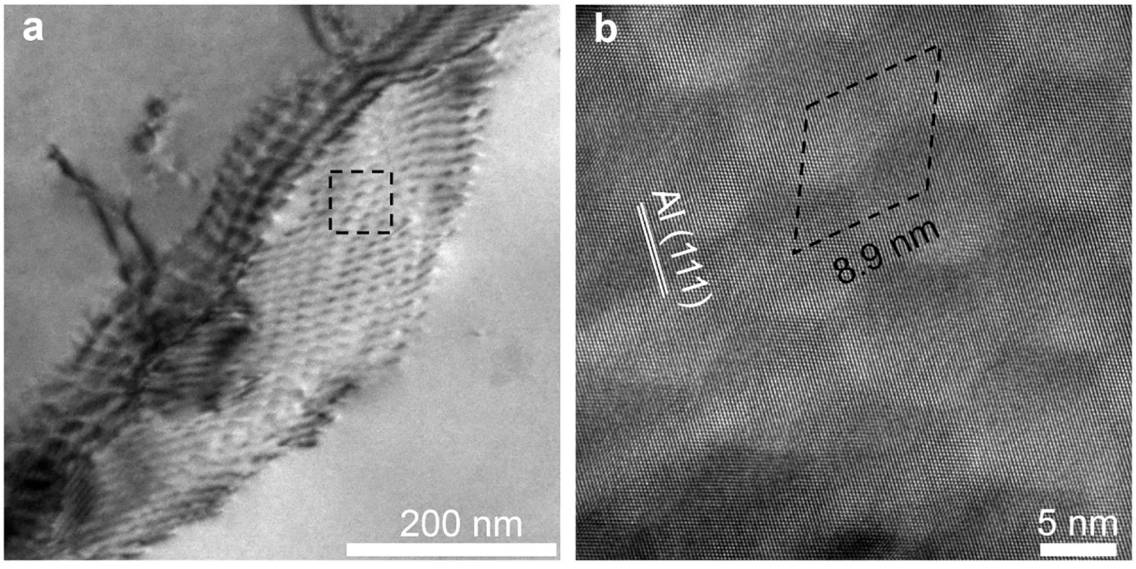

Fig. 1. TEM observation of interface structure. (a) The interface microstructure between graphene and Al (111). (b) High resolution TEM of selected region in (a). And the periodicity of the moiré pattern for graphene and Al (111) is ~8.9 nm.

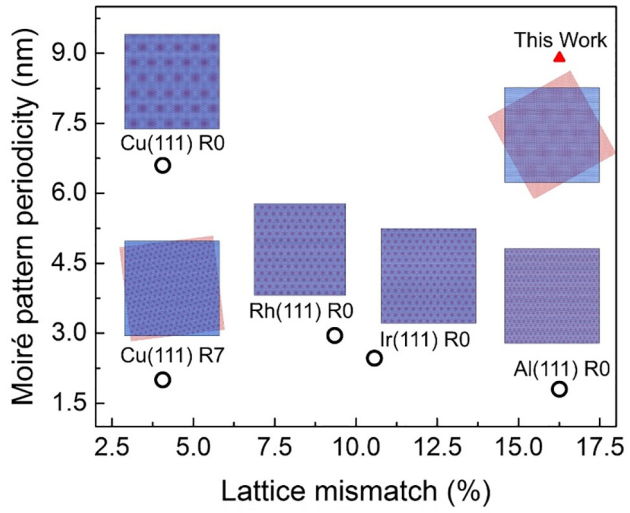

Fig. 2. The variation of moiré pattern periodicity according to lattice mismatch. Rotation 0 degree is simplified as R0 and the other uses the same notation. R0 represents the rotation angle between graphene and metal matrix. The moiré pattern of graphene/Cu (111) interface is in Ref [20]; The moiré pattern of graphene/Rh (111) interface is in Ref [59]; The moiré pattern of graphene/Ir (111) interface is in Ref [29, 58].

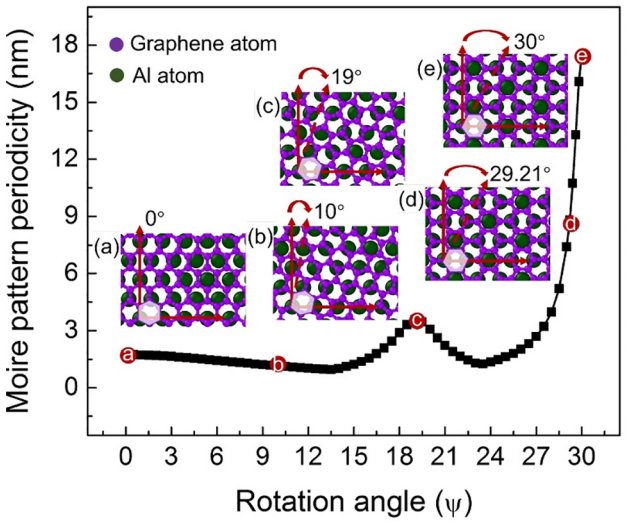

Fig. 3. The moiré pattern periodicity varies with rotation angle via theory calculation. Insets (a)–(e) show interface rotation details. Green atoms represent Al atoms, purple atoms represent graphene atoms, and the radius of Al and graphene atoms are reduced to 1 and 0.5 Å, respectively. Semitransparent purple hexagon and rotation angle are plotted for guidance and clear observation.

the several rotation positions correlated between Al and graphene layer, rotational hexagons in semitransparent purple are labelled for guidance. Specifically, the interface configurations at rotation angle of 0°, 10°, 19°, 29.21° and 30° are estimated to be 1.74 nm, 1.15 nm, 3.57 nm, 8.90 nm and 17.47 nm, respectively, based on theory calculations shown in Fig. S8.

3.3. MD simulations of moiré pattern formation process and mechanism

The moiré pattern periodicity depends on the in-plane rotation angle of the graphene layer with respect to the Al (111) matrix. To further explore the moiré pattern formation mechanism determinate by fabrication technique, MD simulations were performed as shown in Fig. 4. Considering the circumstance that present Al powders have melted while graphene still remains solid state, in addition to literatures reported graphene growth dynamics and the various moiré pattern interface are temperature and pressure dependent [57,60], so cooling velocity rather fusing temperature acts as a controllable parameter and is selected as the crucial variation in forming the graphene/Al interface in present study. Then, the moiré pattern interface formation model with regard to cooling/solidification molten Al is proposed as shown in Figs. S3-S4, and the interfacial moiré pattern formation process and underlying mechanism in the graphene/Al system are shown in Fig. 4. Specifically, the temperature of system decreases from 1200 K to 10 K in 195 ps at a cooling rate of 6.1 K/ps. Numerous formation processes with different cooling rates have also been simulated, together with the animation under the cooling rate of 6.1 K/ps are presented in Supplementary Information S2. From the snapshots, potential energy of Al atoms decreases at reduced temperature as shown in colored atoms in Fig. 4(a), showing Al atoms organized over the graphene substrate (purple atoms) to achieve order state. Eventually, polycrystalline Al grains appear on graphene substrate at 10 K, indicating distinct graphene/Al interfaces based on various rotation orientations were formed. The rotation angles of the aforementioned crystalline grains labelled as A, B, C and D domains are 19.6–21.3, 21.9–22.4, 11.3–11.7 and 28.55–29.11 degrees, respectively. Furthermore, the last figure in Fig. 4(a) shows the enlarged rectangle view of the top view snapshot at 10 K, demonstrating the ~29 degree rotation domain. This rotation orientation interface is very close to the theoretical rotation angle for the moiré pattern morphology obtained experimentally shown in Fig. 1.

By conducting MD simulations, as discussed before, the experimentally observed ~8.9 nm periodic moiré pattern can be obtained by cooling/solidifying at a cooling rate of 6.1 K/ps, which is much higher than the cooling rate reported previously [54,61]. From this, thermal stress raises upon rapid cooling. Therefore, thermal stress upon rapid cooling may be the cause of the ~8.9 nm periodic moiré pattern interface shown in Fig. 1, which is also consistent with the fabrication method of suction casting with rapidly solidified characteristic. In addition, by adjusting cooling velocity (as described in Supplementary Information S2), the graphene/Al interfaces could exhibit distinct moiré pattern characteristics. Overall, it can be inferred that the moiré pattern of different periodicities can be obtained by adjusting the cooling rate to form different magnitudes of thermal stress, thus result in stimulated rotational growth of the molten metal. The corresponding schematic diagram of formation mechanism is depicted in the upper part of Fig. 4(b), showing adjusting cooling rate induced thermal stress stimulus is supposed to lead to variation in moiré pattern periodicity. The top views in Fig. 4(b) show the moiré pattern characteristics of R0 and R29.21 interface. It can be clearly seen that the morphology and periodicity of the moiré pattern rotated by 29.21° are completely consistent with the moiré pattern observed in the experiment. Black rhombus and letter "P" are labelled to represent the periodicity. In addition, rhombus sizes in the former and the latter indicate five-fold and unit moiré pattern periodicity, respectively.

3.4. MD simulations of graphene/Al interface and the work of adhesion

Since the knowledge of interface interaction associated with moiré pattern at graphene/Al interface would shed light on that in bulk systems, especially their atomic/electronic structures. Hence, it is necessary to interpret the moiré pattern interface derived in the graphene/Al composite, the moiré pattern related interface interactions were investigated by MD simulations in present study for basic understanding. The top views of graphene/Al (111) interface energy distribution at R0 and R29.21 corresponding to the one with ~8.9 nm moiré pattern periodicity are shown in Figs. 5(a) and 5(b), in which graphene atoms are colored from blue to red based on their potential energy, and Al atoms are

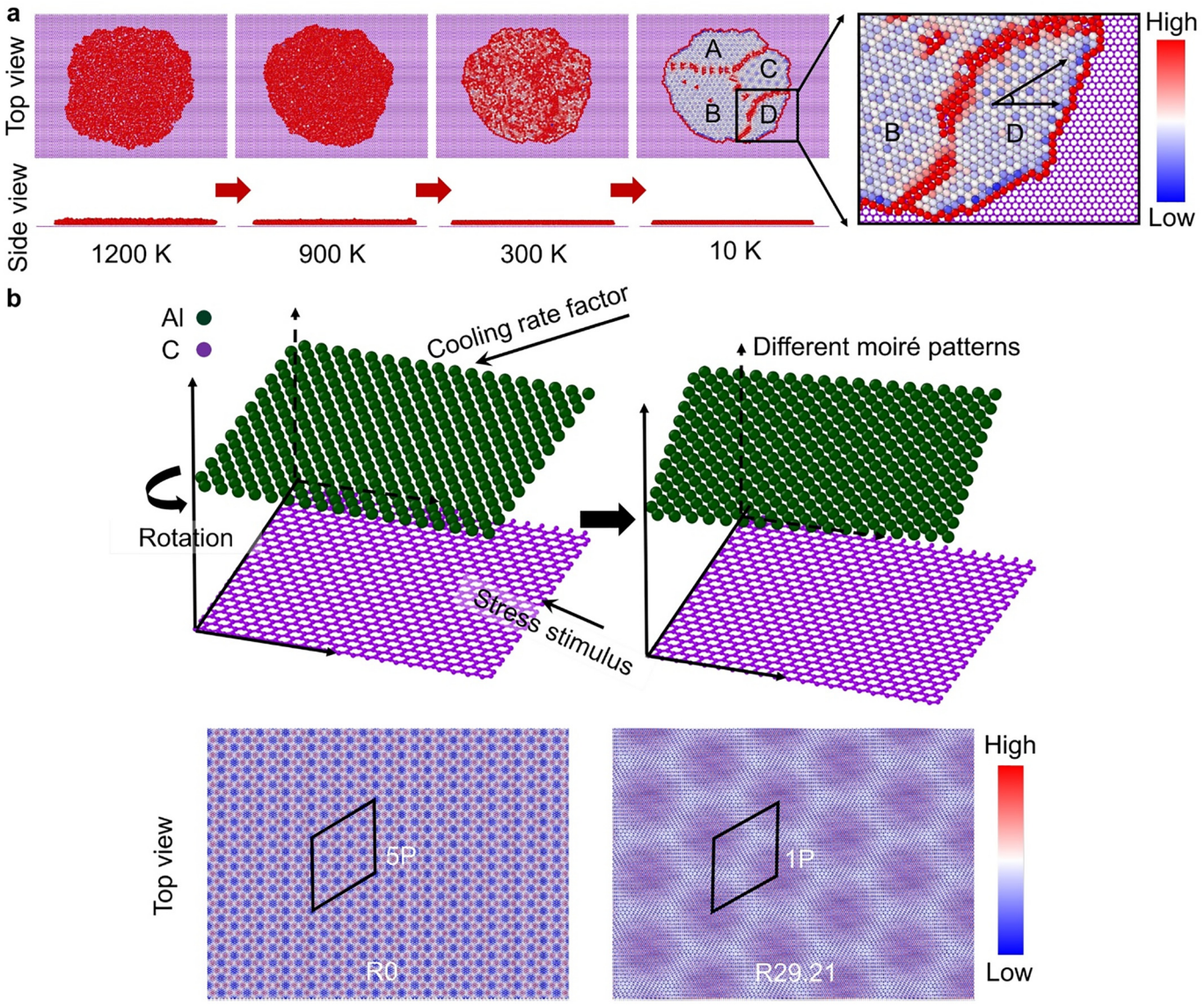

Fig. 4. The interfacial moiré pattern formation process and mechanism in graphene/Al systems. (a) The temperature of system decreases from 1200 K to 10 K in 195 ps during the cooling process. Several rotation orientation graphene/Al interfaces are formed labelled as A, B, C and D domains in the last step, and the last figure is the enlarged rectangle view in (a). Al atoms are colored by potential energy and only graphene (purple) atoms are reduced to 0.5 Å for convenient observation. (b) The schematic diagram of interfacial moiré pattern formation mechanism. Green and purple atoms indicate Al atoms and graphene substrate respectively. The top views in the lower part show the moiré pattern characteristics of R0 and R29.21 interface, through potential energy coloring of the graphene layer. Letter "P" means periodicity so that rhombus sizes indicate five-fold and unit moiré pattern periodicity respectively.

depicted in green. Deep analysis, the interface energy difference between the two interfaces derived at R0 and R29.21, together with the interfacial moiré pattern periodicity should be attributed to the different stacking arrangement of the graphene lattice over the Al (111) lattice, origin from lattice/rotation angle mismatch. The white circles and rectangles in the figures correspond to similar locations but show different stacking of atomic structures (details described in Supplementary Information S4), consequently, R29.21 interface exhibits different interface energy state unlike the common sense of that at R0 interface. Besides, the unit moiré pattern periodicity marked by rhombus has been intriguingly identified to be closely correlated to the variation trend of interface energy distribution, namely, variation in interface interaction. This is confirmed by the literature that the interaction between graphene and metal (111) interface changes depending on the interface structure [28,45] that play a crucial role in determining the electronic properties of the inserted graphene. Especially as literatures about the adsorption of graphene to metal (111) surfaces reported that the rotational orientation of graphene is found to strongly affect its interaction with the substrate [41,62], e.g., the distinguishable extent of charge transfer from the Al to the graphene layer with different stacking arrangements at R0 interface. Therefore, it is worth noting that the interface stacking discrepancy between the two interfaces at 0° and 29.21° rotation cannot be ignored since the electronic properties of graphene are easily influenced by interface interactions corresponding to the interface stacking.

Furthermore, the moiré pattern interface is discussed from the perspective of the interface work function, which is considered closely related to interfacial electronic/magnetic properties as revealed by domain orientation dependent graphene electronics in graphene/Pd (111) [24]. Then, the interface work function of above two interfaces are calculated, and detailed models and calculation methods are shown in Fig. S6. Specifically, the work of adhesion herein is defined as:

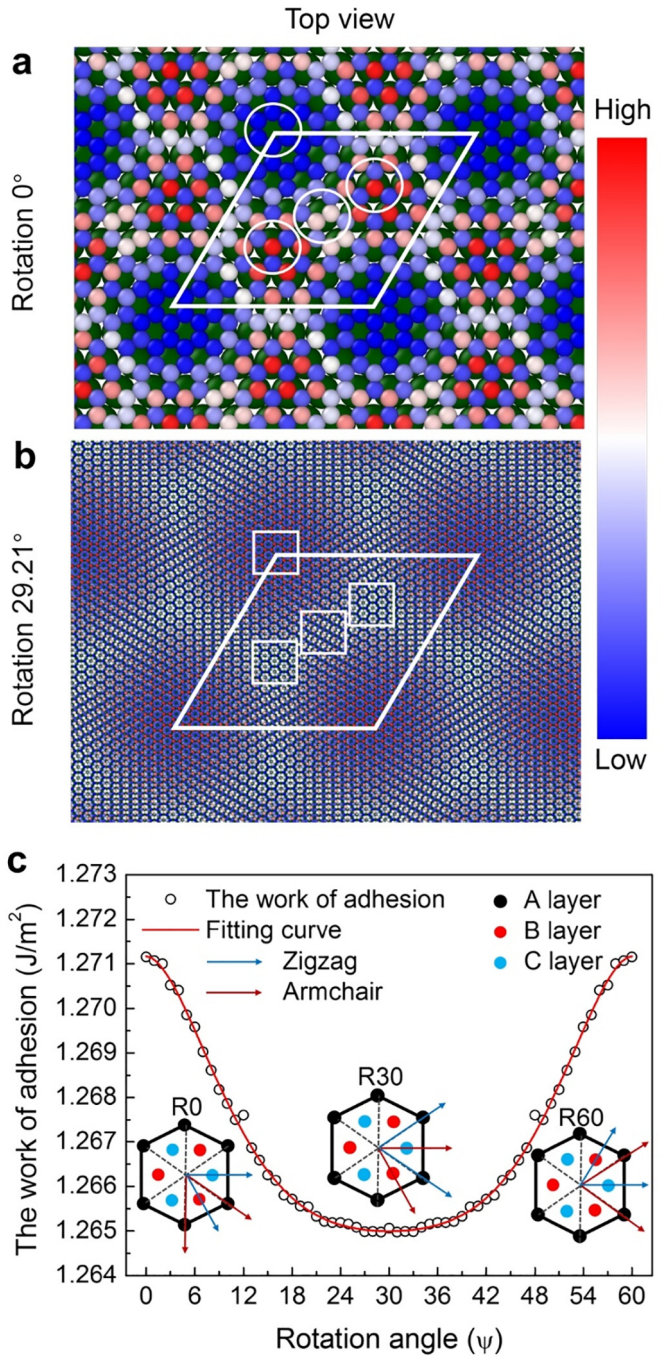

Fig. 5. The interfacial atomic structures and interface interactions at graphene/Al (111) interface. (a) Top views of graphene/Al (111) interface energy distribution at typical and experimental rotation angles of 0° and 29.21° after relaxation. Graphene atoms are colored by potential energy. Green atoms indicate Al atoms. The rhombus means unit moiré pattern periodicity. (b) The rotation angle dependence of the work of adhesion. The insets show simplified interface configuration under three rotation angles R0, R30 and R60. Black, red and blue atoms indicate the stacking of Al layer. Red and blue arrows indicate armchair and zigzag directions of graphene layer.

$$W_{ad} = (E_{separate-Al/graphene} - E_{together-Al/graphene})/A = \gamma_{A1(111)} + \gamma_{graphene} - E_{Int} \quad (1)$$

where $E_{separate\text{-}A1/graphene}$ is total energy of separate A1 and graphene model, $E_{together\text{-}Al/graphene}$ is the total energy of the graphene/A1 model, A represents graphene/a1 interface area, $\gamma_{A1(111)}$, $\gamma_{graphene}$ is the surface energy of A1 and graphene model, respectively, and E_{Int} is interface energy. According to Eq. (1), the interface energy should be inversely proportional to the work of adhesion. As a result, the work of adhesion for R0 and R29.21 are calculated to be 1.271 J/m^2 and 1.265 J/m^2, respectively. Therefore, the moiré pattern periodicity of ~8.9 nm observed experimentally in graphene/A1 interface has a lower work of adhesion, in consistent with large interface energy.

In addition, by adjusting the fabrication conditions, the graphene/Al interface system with a variety of rotation orientations is supposed to be obtained. Thus a deep understanding of the physics and chemistry underpinning graphene/Al interface is fundamental to guide the predictive design for the GRMMCs. Then, sixty graphene/Al (111) interface models are generated by rotating at 1° interval until 60°, for the purpose of interpreting the rotation angle dependent the work of adhesion as shown in Fig. 5(c). As a result, the work of adhesion is evidently reduced with the increase of the rotation angle for R0 to R30, and opposite trend is derived as rotation angles changed from R30 to R60, showing a symmetry at each 30 rotation degree that consisted well with the chirality properties of graphene. The corresponding insets in Fig. 5(c) show the simplified interface configuration under three rotation angles R0, R30 and R60 well, and exhibiting that R0 and R60 have the same interface stacking thus showing the symmetry demonstrated above. Also, the moiré pattern periodicity at each rotation orientation angle after relaxation is obtained (Video S10 in Supplementary Information). Specifically, the periodicities of rotation 0°, 10°, 19°, 29.21° and 30° are about 1.73 nm, 1.12 nm, 3.60 nm, 9.07 nm and 17.29 nm, respectively, which is similar to theoretical periodicity in Fig. 3 but still slightly different. This slight strain matches the previously proposed thermal stress, which contributes to interface rotational growth. Furthermore, there may be another case that the competition relation between lattice misfit and interface rotation or both factors work, which needs future investigation. In addition, as mentioned earlier, the change trend of the work of adhesion with the rotation angle should be opposite to the interface energy. So the interface energy is larger when it is close to 30° and the R29.21 interface is not as stable as the low energy R0 interface, which might be rational for that rapid cooling rate could provide enough energy for forming the interface.

4. Conclusions and outlook

In conclusion, moiré pattern with large periodicity of ~8.9 nm has been discovered at graphene/Al (111) interface fabricated through vacuum arc melting and suction casting technique for the first time. Due to difficulty in investigating the properties of moiré pattern interface experimentally, in this case, through theoretical calculation and simulating computation, it is verified that the moiré pattern periodicity is strongly dependent on rotation angles, which may be induced by thermal stress during cooling process by experiments. Moreover, the obtained ~8.9 nm moiré pattern interface of graphene/Al (111) system is understood from interfacial atomic structures, the work of adhesion and interface energy based on MD simulations, in addition with the possible graphene/Al moiré pattern interface. The understanding of the forming mechanisms and interface interaction of graphene/Al moiré pattern interface is foundational for designing and engineering the physicochemical properties of a plenty of electronic/chemical applications.

We believe that the moiré pattern interface which we have observed could benefit to mechanical/electrical properties. Since a clean interface often means good interface bonding, avoiding forming Al—C compounds that weaken load transfer effect and deteriorate material properties both in mechanics and electricity. This study provides the possibility of diverse graphene/Al interface types for electronic devices or structural materials through tailoring interface structures to realize excellent properties in graphene/Al systems. For example, the R29.21 interface may be in favor of forming plenty of stacking fault/twins during deformation in our progress study, which is helpful to enhance the strength of graphene/Al

composite. A knowledge of the diverse graphene/Al interface related electronic properties can be further studied using density functional theory (DFT) based on experimental parameters presented. Thereafter, another interesting future experiment is the study of precise control of growing graphene/Al film with specific moiré pattern periodicity. Meanwhile, the interfacing of 2D graphene with 3D metals will spark many more novel physicochemical phenomena and functionalities, as well as providing for modern applications, such as next generation electronic devices and advanced nanocomposites.

Credit authorship contribution statement

Shuang Zhang: Methodology, Software, Writing - original draft. **Dongjun He:** Methodology, Writing - original draft. **Ping Huang:** Conceptualization, Writing - review & editing. **Fei Wang:** Conceptualization, Writing - review & editing.

Declaration of Competing Interest

The authors declare no competing financial interest.

Acknowledgements

The present work was supported by the Natural Science Foundation of Shaanxi Province (Nos. 2019TD-020), Natural Science Basic Research Plan in Shaanxi Province of China (No. 2020JM-41, No. 2020JM-33) and the National Natural Science Foundation of China (Grant Nos. 51471131).

Appendix A. Supplementary data

Supplementary data to this article can be found online at https://doi.org/10.1016/j.matdes.2021.109509.

References

[1] C. Lee, X. Wei, J.W. Kysar, J. Hone, Measurement of the elastic properties and intrinsic strength of monolayer graphene, Science. 321 (2008) 385–388, https://doi.org/10.1126/science.1157996.
[2] M. Batzill, The surface science of graphene: metal interfaces, CVD synthesis, nanoribbons, chemical modifications, and defects, Surf. Sci. Rep. 67 (2012) 83–115, https://doi.org/10.1016/j.surfrep.2011.12.001.
[3] J. Scott Bunch, Arend M. van der Zande, Scott S. Verbridge, Ian W. Frank, David M. Tanenbaum, Jeevak M. Parpia, et al., Electromechanical resonators from Graphene sheets, Science. 315 (2007) 490–493, https://doi.org/10.1126/science.1136836.
[4] A.K. Bodenmann, A.H. MacDonald, Graphene: exploring carbon flatland, Phys. Today 60 (2007) 35–41, https://doi.org/10.1063/1.2774096.
[5] K.S. Kim, Y. Zhao, H. Jang, S.Y. Lee, J.M. Kim, K.S. Kim, et al., Large-scale pattern growth of graphene films for stretchable transparent electrodes, Nature. 457 (2009) 706–710, https://doi.org/10.1038/nature07719.
[6] S.C. Tjong, Recent progress in the development and properties of novel metal matrix nanocomposites reinforced with carbon nanotubes and graphene nanosheets, Mater. Sci. Eng. R. Rep. 74 (2013) 281–350, https://doi.org/10.1016/j.mser.2013.08.001.
[7] M. Yortanlı, E. Mete, Common surface structures of graphene and Au(111) the effect of rotational angle on adsorption and electronic properties, J. Chem. Phys. 151 (2019), 214701, https://doi.org/10.1063/1.5127099.
[8] M. Cao, D.B. Xiong, L. Yang, S. Li, Y. Xie, Q. Guo, et al., Ultrahigh electrical conductivity of Graphene embedded in metals, Adv. Funct. Mater. 29 (2019), 1806792, https://doi.org/10.1002/adfm.201806792.
[9] D.G. Papageorgiou, I.A. Kinloch, R.J. Young, Mechanical properties of graphene and graphene-based nanocomposites, Prog. Mater Sci. 90 (2017) 75–127, https://doi.org/10.1016/j.pmatsci.2017.07.004.
[10] J. Wintterlin, M.L. Bocquet, Graphene on metal surfaces, Surf. Sci. 603 (2009) 1841–1852, https://doi.org/10.1016/j.susc.2008.08.037.
[11] Y. Xiao, J. Liu, L. Fu, Moiré is more: access to new properties of two-dimensional layered materials, Matter. 3 (2020) 1142–1161, https://doi.org/10.1016/j.matt.2020.07.001.
[12] M. Yang, Y. Liu, T. Fan, D. Zhang, Metal-graphene interfaces in epitaxial and bulk systems: a review, Prog. Mater. Sci. 110 (2020) 100652, https://doi.org/10.1016/j.pmatsci.2020.100652.
[13] C. Backes, A.M. Abdelkader, C. Alonso, A. Andrieux-Ledier, R. Arenal, J. Azpeitia, et al., Production and processing of graphene and related materials, 2D Mater 7 (2020), 022001, https://doi.org/10.1088/2053-1583/ab1e0a.
[14] S. Carr, S. Fang, E. Kaxiras, Electronic-structure methods for twisted moiré layers, Nat. Rev. Mater. 5 (2020) 748–763, https://doi.org/10.1038/s41578-020-0214-0.
[15] P.S. Mahapatra, B. Ghawri, M. Garg, S. Mandal, K. Watanabe, T. Taniguchi, et al., Misorientation-controlled cross-plane thermoelectricity in twisted bilayer graphene, Phys. Rev. Lett. 125 (2020) 226802, https://doi.org/10.1103/PhysRevLett.125.226802.
[16] Junho Choi, Wei-Ting Hsu, Li-Syuan Lu, Liuyang Sun, Hui-Yu Cheng, Ming-Hao Lee, et al., Moiré potential impedes interlayer exciton diffusion in van der Waals heterostructures, Sci. Adv. 6 (2020), eaba8866, https://doi.org/10.1126/sciadv.aba8866.
[17] Y. Cao, V. Fatemi, S. Fang, K. Watanabe, T. Taniguchi, E. Kaxiras, et al., Unconventional superconductivity in magic-angle graphene superlattices, Nature. 556 (2018) 43–50, https://doi.org/10.1038/nature26160.
[18] H. Tetlow, J. Posthuma de Boer, I.J. Ford, D.D. Vvedensky, J. Coraux, L. Kantorovich, Growth of epitaxial graphene: theory and experiment, Phys. Rep. 542 (2014) 195–295, https://doi.org/10.1016/j.physrep.2014.03.003.
[19] P. Süle, M. Szendrő, C. Hwang, L. Tapasztó, Rotation misorientated graphene moiré superlattices on Cu (111): classical molecular dynamics simulations and scanning tunneling microscopy studies, Carbon. 77 (2014) 1082–1089, https://doi.org/10.1016/j.carbon.2014.06.024.
[20] L. Gao, J.R. Guest, N.P. Guisinger, Epitaxial graphene on Cu(111), Nano Lett. 10 (2010) 3512–3516, https://doi.org/10.1021/nl1016706.
[21] Z. Zou, V. Carnevali, M. Jugovac, L.L. Patera, A. Sala, M. Panighel, et al., Graphene on nickel (100) micrograins: modulating the interface interaction by extended moiré superstructures, Carbon. 130 (2018) 441–447, https://doi.org/10.1016/j.carbon.2018.01.010.
[22] L.G. Salamanca-Riba, R.A. Isaacs, M.C. LeMieux, J. Wan, K. Gaskell, Y. Jiang, et al., Synthetic crystals of silver with carbon: 3D Epitaxy of carbon nanostructures in the silver lattice, Adv. Funct. Mater. 25 (2015) 4768–4777, https://doi.org/10.1002/adfm.201501156.
[23] A. Palinkas, P. Süle, M. Szendro, G. Molnar, C. Hwang, L.P. Biro, et al., Moire superlattices in strained graphene-gold hybrid nanostructures, Carbon. 107 (2016) 792–799, https://doi.org/10.1016/j.carbon.2016.06.081.
[24] Y. Murata, E. Starodub, B.B. Kappes, C.V. Ciobanu, N.C. Bartelt, K.F. McCarty, et al., Orientation-dependent work function of graphene on Pd(111), Appl. Phys. Lett. 97 (2010)https://doi.org/10.1063/1.3495784.
[25] P. Merino, M. Švec, A.L. Pinardi, G. Otero, J.A. Martín-Gago, Strain-driven moiré superstructures of epitaxial graphene on transition metal surfaces, Acs Nano 5 (2011) 5627–5634, https://doi.org/10.1021/nn201200j.
[26] B. Sun, W. Ouyang, J. Gu, C. Wang, J. Wang, L. Mi, Formation of Moiré superstructure of epitaxial graphene on Pt(111): a molecular dynamic simulation investigation, Mater. Chem. Phys. 253 (2020), 123126, https://doi.org/10.1016/j.matchemphys.2020.123126.
[27] P.L. Muriel Sicot, Andreas Zusan, Samuel Bouvron, Ole Zander, Martin Weser, Yuriy S. Dedkov, Karsten Horn, Mikhail Fonin, Size-Selected Epitaxial Nanoislands Underneath Graphene Moiré on Rh(111), ACS Nano 6 (2012) 151–158, https://doi.org/10.1021/nn203169j.
[28] A. Holtsch, T. Euwens, B. Uder, S. Grandthyll, F. Müller, U. Hartmann, Analysis of atomic Moiré patterns on graphene/Rh(1 1 1), Surf. Sci. 668 (2018) 107–111, https://doi.org/10.1016/j.susc.2017.10.026.
[29] K.M. Omambac, H. Hattab, C. Brand, G. Jnawali, A.T. N'Diaye, J. Coraux, et al., Temperature-controlled rotational Epitaxy of Graphene, Nano Lett. 19 (2019) 4594–4600, https://doi.org/10.1021/acs.nanolett.9b01565.
[30] A. Varykhalov, O. Rader, Graphene grown on Co(0001) films and islands: Electronic structure and its precise magnetization dependence, Phys. Rev. B. 80 (2009) https://doi.org/10.1103/PhysRevB.80.035437.
[31] S. Lizzit, R. Larciprete, P. Lacovig, M. Dalmiglio, F. Orlando, A. Baraldi, et al., Transfer-free electrical insulation of epitaxial graphene from its metal substrate, Nano Lett. 12 (2012) 4503–4507, https://doi.org/10.1021/nl301614j.
[32] P. Zeller, Sebastian Günther, What are the possible moiré patterns of graphene on hexagonally packed surfaces? Universal solution for hexagonal coincidence lattices, derived by a geometric construction, New J. Phys 16 (8) (2014) https://doi.org/10.1088/1367-2630/16/8/083028.
[33] S. Günther, P. Zeller, Moiré Patterns of Graphene on Metals, Encyclopedia of Interfacial Chemistry, 2018 295–307.
[34] M. Cao, Y. Luo, Y. Xie, Z. Tan, G. Fan, Q. Guo, et al., The Influence of Interface Structure on the Electrical Conductivity of Graphene Embedded in Aluminum Matrix, Adv. Mater. Interfaces 6 (2019) https://doi.org/10.1002/admi.201900468.
[35] Z. Li, Q. Guo, Z. Li, G. Fan, D.B. Xiong, Y. Su, et al., Enhanced mechanical properties of Graphene (reduced Graphene oxide)/aluminum composites with a bioinspired Nanolaminated structure, Nano Lett. 15 (2015) 8077–8083, https://doi.org/10.1021/acs.nanolett.5b03492.
[36] Z. Hu, G. Tong, D. Lin, C. Chen, H. Guo, J. Xu, et al., Graphene-reinforced metal matrix nanocomposites – a review, Mater. Sci. Technol. 32 (2016) 930–953, https://doi.org/10.1080/02670836.2015.1104018.
[37] S. Wang, X. Wei, J. Xu, J. Hong, X. Song, C. Yu, et al., Strengthening and toughening mechanisms in refilled friction stir spot welding of AA2014 aluminum alloy reinforced by graphene nanosheets, Mater. Des. 186 (2020) 108212, https://doi.org/10.1016/j.matdes.2019.108212.
[38] Y. Jiang, Z. Tan, G. Fan, L. Wang, D.-B. Xiong, Q. Guo, et al., Reaction-free interface promoting strength-ductility balance in graphene nanosheet/Al composites, Carbon. 158 (2020) 449–455, https://doi.org/10.1016/j.carbon.2019.11.010.
[39] Z. Yu, W. Yang, C. Zhou, N. Zhang, Z. Chao, H. Liu, et al., Effect of ball milling time on graphene nanosheets reinforced Al6063 composite fabricated by pressure infiltration method, Carbon 141 (2019) 25–39, https://doi.org/10.1016/j.carbon.2018.09.041.
[40] J.A. Robinson, M. LaBella, M. Zhu, M. Hollander, R. Kasarda, Z. Hughes, et al., Contacting graphene, Appl. Phys. Lett. 98 (2011), 053103, https://doi.org/10.1063/1.3549183.
[41] M.S. Christian, A. Otero-de-la-Roza, E.R. Johnson, Adsorption of graphene to metal (111) surfaces using the exchange-hole dipole moment model, Carbon. 124 (2017) 531–540, https://doi.org/10.1016/j.carbon.2017.08.077.

[42] E.N. Voloshina, Yu.S. Dedkov, S. Torbrügge, A. Thissen, M. Fonin, Graphene on Rh (111): scanning tunneling and atomic force microscopies studies, Appl. Phys. Lett. 100 (2012) 241606, https://doi.org/10.1063/1.4729549.
[43] B. Wang, M.-L. Bocquet, Monolayer Graphene and h-BN on metal substrates as versatile templates for metallic Nanoclusters, J. Phys. Chem. Lett. 2 (2011) 2341–2345, https://doi.org/10.1021/jz201047c.
[44] M. Iannuzzi, J. Hutter, Comparative study of the nature of chemical bonding of corrugated graphene on Ru(0001) and Rh(111) by electronic structure calculations, Surf. Sci. 605 (2011) 1360–1368, https://doi.org/10.1016/j.susc.2011.04.031.
[45] E. Starodub, A. Bostwick, L. Moreschini, S. Nie, F.E. Gabaly, K.F. McCarty, et al., In-plane orientation effects on the electronic structure, stability, and Raman scattering of monolayer graphene on Ir(111), Phys. Rev. B 83 (2011) https://doi.org/10.1103/PhysRevB.83.125428.
[46] X. Zhang, J. Zhou, H. Song, X. Chen, Y.V. Fedoseeva, A.V. Okotrub, et al., "Butterfly effect" in CuO/graphene composite nanosheets: a small interfacial adjustment triggers big changes in electronic structure and Li-ion storage performance, ACS Appl. Mater. Inter. 6 (2014) 17236–17244, https://doi.org/10.1021/am505186a.
[47] Z. Xu, G. Zhao, L. Qiu, X. Zhang, G. Qiao, F. Ding, Molecular dynamics simulation of graphene sinking during chemical vapor deposition growth on semi-molten Cu substrate, npj Comput. Mater. 6 (2020)https://doi.org/10.1038/s41524-020-0281-1.
[48] S. Plimpton, Fast parallel algorithms for short-range molecular-dynamics, J. Comput. Phys. 117 (1995) 1–19, https://doi.org/10.1006/jcph.1995.1039.
[49] M.I. Mendelev, M.J. Kramer, C.A. Becker, M. Asta, Analysis of semi-empirical interatomic potentials appropriate for simulation of crystalline and liquid Al and cu, Philos. Mag. 88 (2008) 1723–1750, https://doi.org/10.1080/14786430802206482.
[50] C.R. Dandekar, Y.C. Shin, Molecular dynamics based cohesive zone law for describing Al–SiC interface mechanics, Composites Part A. 42 (2011) 355–363, https://doi.org/10.1016/j.compositesa.2010.12.005.
[51] S.J. Stuart, A.B. Tutein, J.A. Harrison, A reactive potential for hydrocarbons with intermolecular interactions, J. Chem. Phys. 112 (2000) 6472–6486, https://doi.org/10.1063/1.481208.
[52] J.-Q. Zhu, X. Liu, Q.-S. Yang, Dislocation-blocking mechanism for the strengthening and toughening of laminated graphene/Al composites, Comput. Mater. Sci. 160 (2019) 72–81, https://doi.org/10.1016/j.commatsci.2018.12.061.
[53] A. Stukowski, Visualization and analysis of atomistic simulation data with OVITO–the open visualization tool, Model. Simul. Mater. Sci. Eng. 18 (2010), 015012, https://doi.org/10.1088/0965-0393/18/1/015012.
[54] X. Zhou, X. Liu, J. Lei, Q. Yang, Atomic simulations of the formation of twist grain boundary and mechanical properties of graphene/aluminum nanolaminated composites, Comput. Mater. Sci. 172 (2020) 109342, https://doi.org/10.1016/j.commatsci.2019.109342.
[55] X. Zhang, N. Zhao, C. He, The superior mechanical and physical properties of nanocarbon reinforced bulk composites achieved by architecture design – a review, Prog. Mater. Sci. 113 (2020) 100672, https://doi.org/10.1016/j.pmatsci.2020.100672.
[56] K. Hermann, Periodic overlayers and moire patterns: theoretical studies of geometric properties, J Phys. Condens. Matter. 24 (2012) 314210, https://doi.org/10.1088/0953-8984/24/31/314210.
[57] J. Zhang, L. Lin, K. Jia, L. Sun, H. Peng, Z. Liu, Controlled growth of single-crystal Graphene films, Adv. Mater. 32 (2020), 1903266, https://doi.org/10.1002/adma.201903266.
[58] H. Hattab, A.T. N'Diaye, D. Wall, C. Klein, G. Jnawali, J. Coraux, et al., Interplay of wrinkles, strain, and lattice parameter in graphene on iridium, Nano Lett. 12 (2012) 678–682, https://doi.org/10.1021/nl203530t.
[59] B. Wang, M. Caffio, C. Bromley, H. Früchtl, R. Schaub, Coupling epitaxy, chemical bonding, and work function at the local scale in transition metal-supported graphene, ACS Nano 4 (2010) 5773–5782, https://doi.org/10.1021/nn101520k.
[60] D. Lin, C. Richard Liu, G.J. Cheng, Single-layer graphene oxide reinforced metal matrix composites by laser sintering: microstructure and mechanical property enhancement, Acta Mater. 80 (2014) 183–193, https://doi.org/10.1016/j.actamat.2014.07.038.
[61] S. Kumar, Graphene Engendered aluminium crystal growth and mechanical properties of its composite: an atomistic investigation, Mater. Chem. Phys. 208 (2018) 41–48, https://doi.org/10.1016/j.matchemphys.2018.01.013.
[62] M.S. Christian, A. Otero-de-la-Roza, E.R. Johnson, Adsorption of graphene to nickel (111) using the exchange-hole dipole moment model, Carbon. 118 (2017) 184–191, https://doi.org/10.1016/j.carbon.2017.03.024.